IMMUNOLOGY

Kisspeptin/GPR54 signaling restricts antiviral innate immune response through regulating calcineurin phosphatase activity

Hongjun Huang[1]*, Qingqing Xiong[1]*, Ning Wang[1]*, Ruoyu Chen[1], Hua Ren[1], Stefan Siwko[2], Honghui Han[3], Mingyao Liu[1,2], Min Qian[1†], Bing Du[1†]

G protein–coupled receptor 54 (GPR54), the key receptor for the neuropeptide hormone kisspeptin, plays essential roles in regulating puberty development and cancer metastasis. However, its role in the antiviral innate immune response is unknown. We report that virus-induced type I interferon (IFN-I) production was significantly enhanced in *Gpr54*-deficient cells and mice and resulted in restricted viral replication. We found a marked increase of kisspeptin in mouse serum during viral infection, which, in turn, impaired IFN-I production and antiviral immunity through the GPR54/calcineurin axis. Mechanistically, kisspeptin/GPR54 signaling recruited calcineurin and increased its phosphatase activity to dephosphorylate and deactivate TANK [tumor necrosis factor receptor-associated factor (TRAF) family member-associated NF-κB activator]–binding kinase 1 (TBK1) in a Ca^{2+}-dependent manner. Thus, our data reveal a kisspeptin/GPR54/calcineurin-mediated immune evasion pathway exploited by virus through the negative feedback loop of TBK1 signaling. These findings also provide insights into the function and cross-talk of kisspeptin, a known neuropeptide hormone, in antiviral innate immune response.

INTRODUCTION

As the first defense against invading viruses, the innate immune system initiates a series of signaling events inducing type I interferon (IFN-I) through pattern recognition receptors, which mainly include the Toll-like receptor (TLR) family, the retinoic acid–inducible gene I (RIG-I)–like receptor (RLR) family, and cytoplasmic DNA receptors (CDRs). Among them, TLR3, TLR7, TLR8, and TLR9 detect viral nucleic acids in the endosome, whereas RLRs and CDRs sense viral nucleic acids in the cytoplasm (*1*). The released IFN-I further activates downstream signaling pathways that lead to the transcriptional induction of hundreds of IFN-stimulated genes to elicit a systemic antiviral response through various mechanisms (*2*). Insufficient IFN-I production causes chronic infection, whereas excessive IFN-I leads to unwanted tissue damage (*3*). Thus, IFN-I signaling must be spatially and temporally orchestrated to avoid immune dysfunction.

TANK [tumor necrosis factor receptor-associated factor (TRAF) family member-associated NF-κB activator]–binding kinase 1 (TBK1) is a central player in initiating IFN-I and the antiviral innate immune response to both RNA and DNA viruses (*4*). TBK1 activation is tightly regulated by posttranslational regulation such as protein phosphorylation and ubiquitination. For example, upon viral infection, TBK1 undergoes self-association and autophosphorylation at Ser^{172} with the help of glycogen synthase kinase-3β (GSK3β) (*5*). TBK1 can also be activated through K63-linked ubiquitination mediated by MIB1 (mind bomb E3 ligase 1), MIB2 (*6*), NRDP1 (neuregulin receptor degradation protein 1) (*7*), or RNF128 (ring finger protein 128) (*8*). Furthermore, the activation of TBK1 is also negatively regulated by the phosphatases PPM1A (protein phosphatase magnesium-dependent 1A) (*9*, *10*), PPM1B (*11*), and PP4 (*12*), as well as the deubiquitinating enzymes CYLD (cylindromatosis) (*13*) and USP2b (ubiquitin-specific protease 2b) (*14*). However, the regulation of TBK1 by extracellular hormonal signals and membrane receptors is poorly understood.

As the most diverse class of sensory receptors, G protein–coupled receptors (GPCRs) can recognize many extracellular stimuli, such as neurotransmitters, hormones, ions, amino acids, and even light (*15*, *16*). Many GPCRs play an important role in surveillance and modulating the immune response. Apart from the classic chemokine receptors, more and more GPCRs including free fatty acid receptors (*17*), purinergic receptors (*18*), adenosine receptors (*19*), dopamine receptors (*20*), and bile acid receptors (*21*) have been found to play nonredundant roles in the immune response. However, relatively little is known about the GPCRs involved in antiviral immune response. As a classic GPCR, GPR54 was not only discovered as a suppressor of cancer metastasis (*22*) but also controls the development of puberty and the reproductive system (*23*, *24*). Binding of the GPR54 ligand kisspeptin results in the activation of different downstream pathways, including the $G_{\alpha q}$/intracellular calcium ions (Ca^{2+}), mitogen-activated protein kinase, and phosphatidylinositol 3-kinase/AKT pathways, in a tissue-specific manner (*25*). Several papers have suggested a role for kisspeptin/GPR54 in immune regulation in response to lipopolysaccharide (LPS)–induced immune stress (*26*) or during pregnancy (*27*). However, the role of kisspeptin/GPR54 in innate immunity and host defense against infection by viral pathogens remains unknown.

Here, we demonstrated that kisspeptin/GPR54 signaling forms a negative feedback loop to limit TBK1 signaling and IFN-I expression in a calcineurin-dependent manner, which may help virus to escape immune elimination. Our results also provide mechanistic insight into the negative regulation of antiviral innate immune response by the neuroendocrine system through kisspeptin/GPR54/calcineurin axis–mediated posttranslational modification of TBK1.

[1]Shanghai Key Laboratory of Regulatory Biology, Institute of Biomedical Sciences and School of Life Sciences, East China Normal University, Shanghai 200241, China. [2]Institute of Biosciences and Technology, Department of Molecular and Cellular Medicine, Texas A&M University Health Science Center, Houston, TX 77030, USA. [3]Shanghai Bioray Laboratories Inc., Shanghai 200241, China.
*These authors contributed equally to this work.
†Corresponding author. Email: bdu.ecnu@gmail.com (B.D.); mqian@bio.ecnu.edu.cn (M.Q.)

RESULTS

GPR54 modulates IFN-I signaling

To investigate the role of kisspeptin/GPR54 signaling in antiviral innate immunity, we constructed *Gpr54*-deficient (*Gpr54*$^{-/-}$) mice (fig. S1A). We infected peritoneal macrophages (PEMs) from *Gpr54*$^{+/+}$ and *Gpr54*$^{-/-}$ mice with the RNA virus vesicular stomatitis virus (VSV) to detect the expression of IFN-I. We found that the expression of *Ifn*-β (both mRNA and protein) and IFN-inducible *Ifn*-α*4* was significantly higher in *Gpr54*-deficient PEMs than in their wild-type counterparts (Fig. 1, A and B). Also, VSV-induced *Ifn*-β was dose-dependent (fig. S1B). It has been shown that intracellular RNA virus is mainly recognized by RIG-I to produce IFN-β, so we transfected PEMs with the RNA viral mimic polyinosinic-polycytidylic acid [poly(I:C)] to explore the influence of GPR54 on RIG-I–associated signaling. As shown in Fig. 1C, intracellular poly(I:C)-induced *Ifn*-β production was enhanced significantly in *Gpr54*-deficient PEMs.

Next, we also sought to determine whether GPR54 is specific for RNA virus or affects the immune response to different classes of viruses. When we infected the *Gpr54*-deficient PEMs with the DNA virus herpes simplex virus type 1 (HSV-1), the production of *Ifn*-β was also increased obviously compared to wild-type PEMs (Fig. 1D). Similar results were also observed in *Gpr54*-deficient bone marrow–derived macrophages (BMMs; Fig. 1, E and F). *Ifn*-β mRNA expression induced by poly(I:C) (a TLR3 ligand), LPS (a TLR4 ligand), imidazoquinoline compound R848 (a TLR7/TLR8 ligand), or the CpG (cytosine phosphate guanosine) oligonucleotide ODN2395 (a TLR9 ligand) was increased in *Gpr54*-deficient PEMs (fig. S1C). Accordingly, the VSV-activated phosphorylation of TBK1 (Ser^{172}) and transcription factor IFN regulatory factor 3 (IRF3; Ser^{396}), which are responsible for initiating the production of IFN-I, was significantly enhanced in *Gpr54*-deficient PEMs (Fig. 1G). Likewise, poly(I:C)- and LPS-induced phosphorylation of TBK1 (Ser^{172}) and

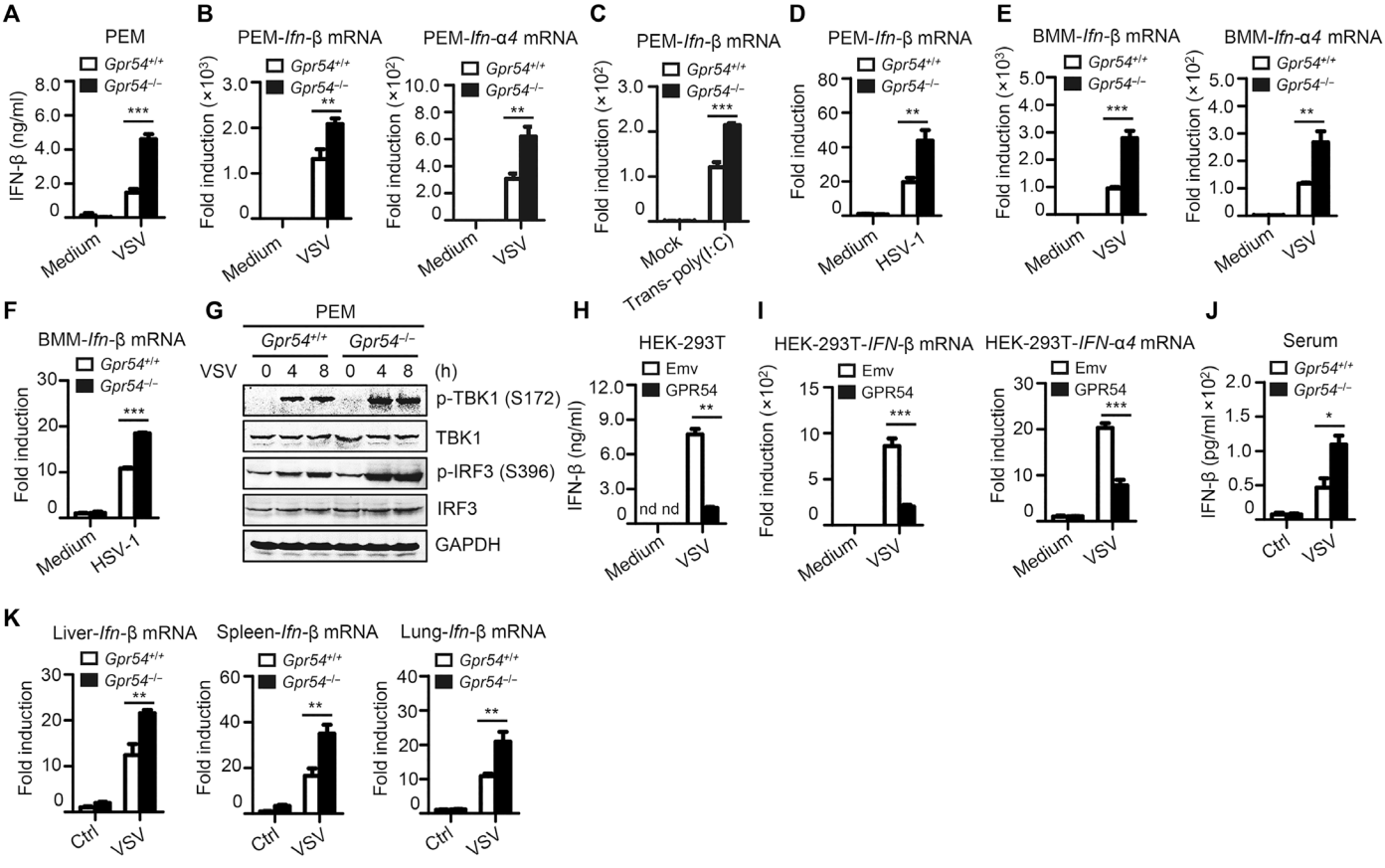

Fig. 1. GPR54 modulates IFN-I signaling. (**A**) Enzyme-linked immunosorbent assay (ELISA) of IFN-β levels in supernatants of *Gpr54*$^{+/+}$ and *Gpr54*$^{-/-}$ PEMs infected with VSV [multiplicity of infection (MOI), 1] for 12 hours. (**B**) Quantitative polymerase chain reaction (qPCR) analysis of *Ifn*-β and *Ifn*-α*4* expression in *Gpr54*$^{+/+}$ and *Gpr54*$^{-/-}$ PEMs infected with VSV (MOI, 1) for 8 hours. (**C**) qPCR analysis of *Ifn*-β expression in *Gpr54*$^{+/+}$ and *Gpr54*$^{-/-}$ PEMs transfected with poly(I:C) (1 μg/ml) for 4 hours. (**D**) qPCR analysis of *Ifn*-β expression in *Gpr54*$^{+/+}$ and *Gpr54*$^{-/-}$ PEMs infected with HSV-1 (MOI, 1) for 8 hours. (**E**) qPCR analysis of *Ifn*-β and *Ifn*-α*4* expression in *Gpr54*$^{+/+}$ and *Gpr54*$^{-/-}$ BMMs infected with VSV (MOI, 1) for 8 hours. (**F**) qPCR analysis of *Ifn*-β expression in *Gpr54*$^{+/+}$ and *Gpr54*$^{-/-}$ BMMs infected with HSV-1 (MOI, 1) for 8 hours. (**G**) Immunoblot analysis of phosphorylated TBK1 and IRF3 or total proteins in lysates of *Gpr54*$^{+/+}$ and *Gpr54*$^{-/-}$ PEMs infected with VSV (MOI, 1) for the indicated times. GAPDH, glyceraldehyde-3-phosphate dehydrogenase. (**H**) ELISA of IFN-β levels in supernatants of *GPR54*-overexpressing HEK-293T (293T) cells infected with VSV (MOI, 1) for 16 hours. Emv, empty vector. (**I**) qPCR analysis of *IFN*-β and *IFN*-α*4* expression in *GPR54*-overexpressing HEK-293T cells infected with VSV (MOI, 1) for 12 hours. (**J**) ELISA of IFN-β levels in sera from *Gpr54*$^{+/+}$ and *Gpr54*$^{-/-}$ mice given intraperitoneal injection of VSV [1 × 10^8 plaque-forming units (PFU) per mouse] for 24 hours. (**K**) qPCR analysis of *Ifn*-β expression in the liver, spleen, and lung from mice in (J). *GAPDH* was used as an internal control for qPCR. Data are representative of three independent experiments (mean ± SD). *P < 0.05, **P < 0.01, ***P < 0.001. nd, not detected.

IRF3 (Ser[396]) was also markedly increased in *Gpr54*-deficient PEMs (fig. S1D). These data indicate that GPR54 regulates IFN-I production in response to a wide range of signals.

To further confirm the influence of GPR54 on IFN-β production, we transiently transfected human embryonic kidney (HEK)–293T cells with green fluorescent protein (GFP)–GPR54 (fig. S1, E and F). We found that VSV-stimulated *IFN*-β (both mRNA and protein) and *IFN*-α*4* expression was markedly impaired in HEK-293T cells transiently expressing GPR54 (Fig. 1, H and I). Consistent with the cellular levels, *Gpr54*-deficient mice produced much more IFN-β in the serum (Fig. 1J), liver, spleen, and lung (Fig. 1K) than did their wild-type littermates in response to infection with VSV. Thus, GPR54 was able to negatively regulate the production of IFN-I in antiviral innate immune response both in vitro and in vivo.

GPR54 negatively regulates host defense against viruses

Since GPR54 is involved in virus-induced IFN-I production, we examined its roles in antiviral response. We challenged PEMs and BMMs with RNA virus VSV or VSV-GFP and found that VSV replication (Fig. 2A) and VSV-GFP infection (Fig. 2B) were also significantly reduced in *Gpr54*-deficient PEMs or BMMs. Moreover, the replication of HSV-1 (Fig. 2, C and D) and Newcastle disease virus (NDV) (Fig. 2E) was also suppressed in *Gpr54*-deficient cells. Furthermore, we transiently expressed GPR54 in HEK-293T cells and found that overexpression of GPR54 facilitated VSV replication in a dose-dependent manner (Fig. 2F). VSV replication in various organs was also significantly lower (Fig. 2G), and lung injury following infection was ameliorated in *Gpr54*-deficient mice compared to controls (Fig. 2H). Consistent with the reduced VSV replication, the survival of *Gpr54*-deficient mice was much greater than of their wild-type littermates (Fig. 2I). Therefore, GPR54 decreased the production of IFN-I and deteriorated the virus-induced tissue damage and mortality.

Kisspeptin restricts virus-induced IFN-I production

As the endogenous ligand of GPR54, *Kiss1*-encoded neuropeptide hormone kisspeptin is mainly expressed in the hypothalamus and pituitary gland of the neuroendocrine system and performs its functions in an autocrine or paracrine manner (*28*). We sought to determine whether kisspeptin functions in regulating the innate immune response to virus infection in a paracrine manner, similar to its role

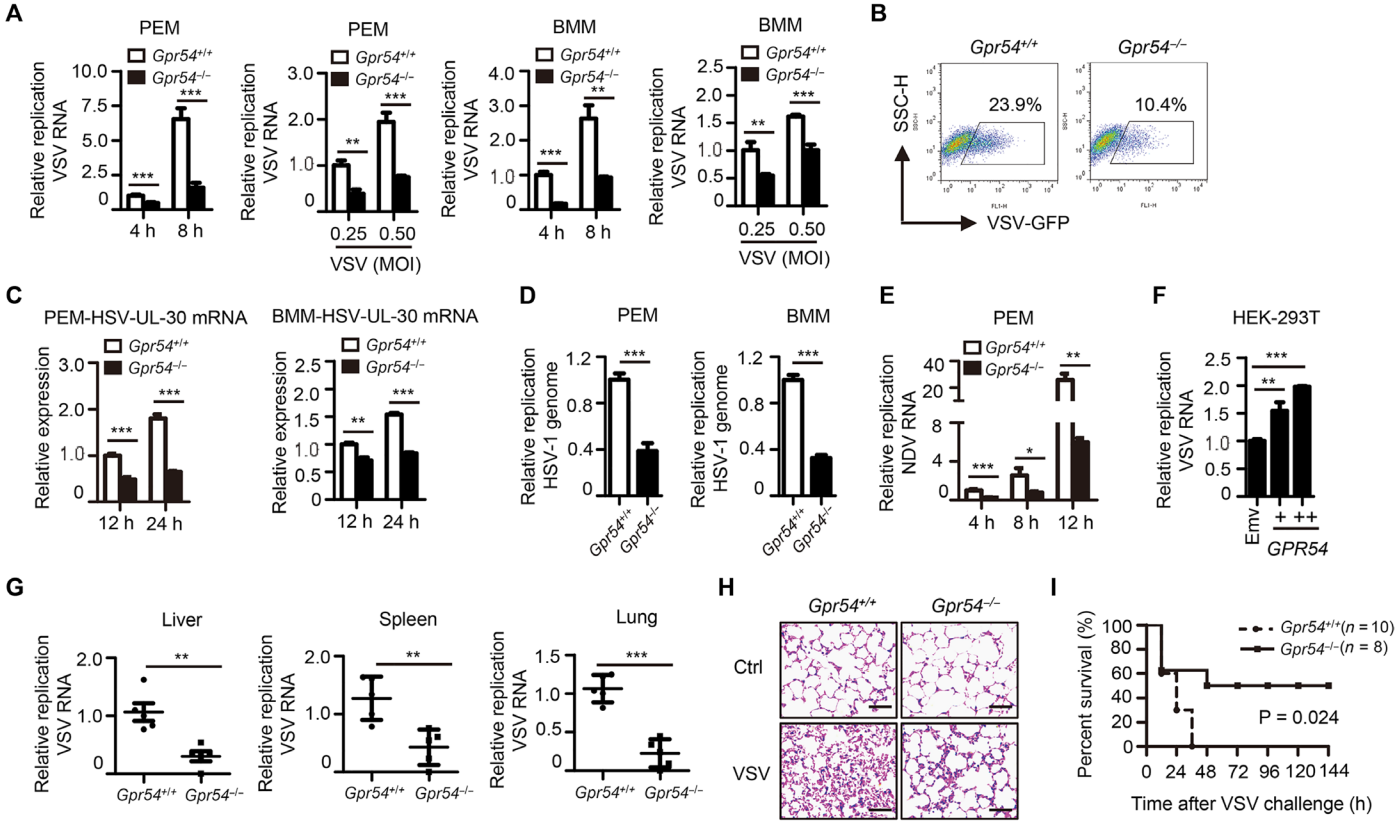

Fig. 2. GPR54 negatively regulates host defense against viruses. (**A**) qPCR analysis of VSV RNA replicates in *Gpr54*$^{+/+}$ and *Gpr54*$^{-/-}$ PEMs or BMMs infected with VSV (MOI, 1) for the indicated times or the indicated VSV MOI for 12 hours. (**B**) PEMs from *Gpr54*$^{+/+}$ and *Gpr54*$^{-/-}$ mice were infected with VSV-GFP (MOI, 0.01) for 12 hours, and VSV-GFP was measured by fluorescence-activated cell sorting (FACS). SSC-H, side scatter-height. (**C**) qPCR analysis of HSV-UL-30 expression in *Gpr54*$^{+/+}$ and *Gpr54*$^{-/-}$ PEMs or BMMs infected with HSV-1 (MOI, 1) for the indicated times. (**D**) qPCR analysis of HSV-1 genomic DNA replicates in *Gpr54*$^{+/+}$ and *Gpr54*$^{-/-}$ PEMs or BMMs infected with HSV-1 (MOI, 1) for 24 hours. (**E**) qPCR analysis of NDV RNA replicates in *Gpr54*$^{+/+}$ and *Gpr54*$^{-/-}$ PEMs infected with NDV (MOI, 1) for the indicated times. (**F**) qPCR analysis of VSV RNA replicates in HEK-293T cells transfected for 28 hours with different amounts (1 and 2 μg) of *GPR54* plasmid and then infected with VSV (MOI, 1) for 12 hours. (**G**) qPCR analysis of VSV RNA replicates in the liver, spleen, and lung from *Gpr54*$^{+/+}$ and *Gpr54*$^{-/-}$ mice infected with VSV (1×10^8 PFU per mouse) intraperitoneally for 24 hours ($n = 5$; mean ± SEM). (**H**) Hematoxylin and eosin staining of lung sections from mice in (G). Scale bars, 200 μm. (**I**) Survival of 8-week-old *Gpr54*$^{+/+}$ and *Gpr54*$^{-/-}$ mice given intraperitoneal injection of VSV (1×10^8 PFU/g) (mean ± SEM). *GAPDH* was used as an internal control for qPCR. Data are representative of three independent experiments (mean ± SD). *$P < 0.05$, **$P < 0.01$, ***$P < 0.001$.

in regulating puberty. First, we checked the expression of *Kiss1* and *Gpr54* in the hypothalamus and pituitary gland of mice following viral infection and found that, although the expression of *Gpr54* (both mRNA and protein) was little changed, the mRNA expression of *Kiss1* and the serum concentration of kisspeptin were both highly increased (Fig. 3, A and B, and fig. S2A). In addition, we also found that the expression of *Kiss1* was increased in other kisspeptin-containing tissues of mice in viral infection (fig. S2B). Although the elevation of *Kiss1* in other kisspeptin-containing tissues does not seem to be as strong as in the hypothalamus and pituitary gland, they may systematically regulate antiviral immune response together with the neuroendocrine organs through kisspeptin in a temporal and spatial context. In contrast, PEMs expressed low levels of *Kiss1*, even in cells infected by VSV (fig. S2C). Furthermore, the expression of *Gpr54* in VSV-, HSV-1–, and IFN-β–treated cells was not significantly changed (fig. S2, D and E), which is consistent with the expression of *GPR54* in hepatitis B virus–infected patients (fig. S2F). The localization of GPR54 on the cell membrane was also unchanged (fig. S2, G and H) during viral infection. These results suggest that, in response to viral infection, kisspeptin is secreted mainly by the neuroendocrine organs in vivo rather than the immune cells.

Next, when we pretreated PEMs with kisspeptin-10 (KP-10; a lower–molecular weight form of endogenous kisspeptin) before VSV or HSV-1 infection to explore the potential role of kisspeptin in viral infection, we found that virus-induced mRNA expression of *Ifn*-β was significantly reduced by KP-10 (Fig. 3C). In accord with this effect on IFN-β expression, the replication of VSV in KP-10 treated cells was increased substantially (Fig. 3D). In addition, KP-10 also significantly suppressed poly(I:C)- and LPS-induced *Ifn*-β production (Fig. 3E), implying that kisspeptin negatively regulates IFN-I. As a classic GPCR, GPR54 couples primarily to $G_{\alpha q/11}$, leading to intracellular Ca^{2+} release and downstream signaling (*25*). Thus, we pretreated the VSV-infected cells with 2-aminoethoxydiphenyl borate (2-APB) to block the release of cytosolic Ca^{2+} and found that VSV

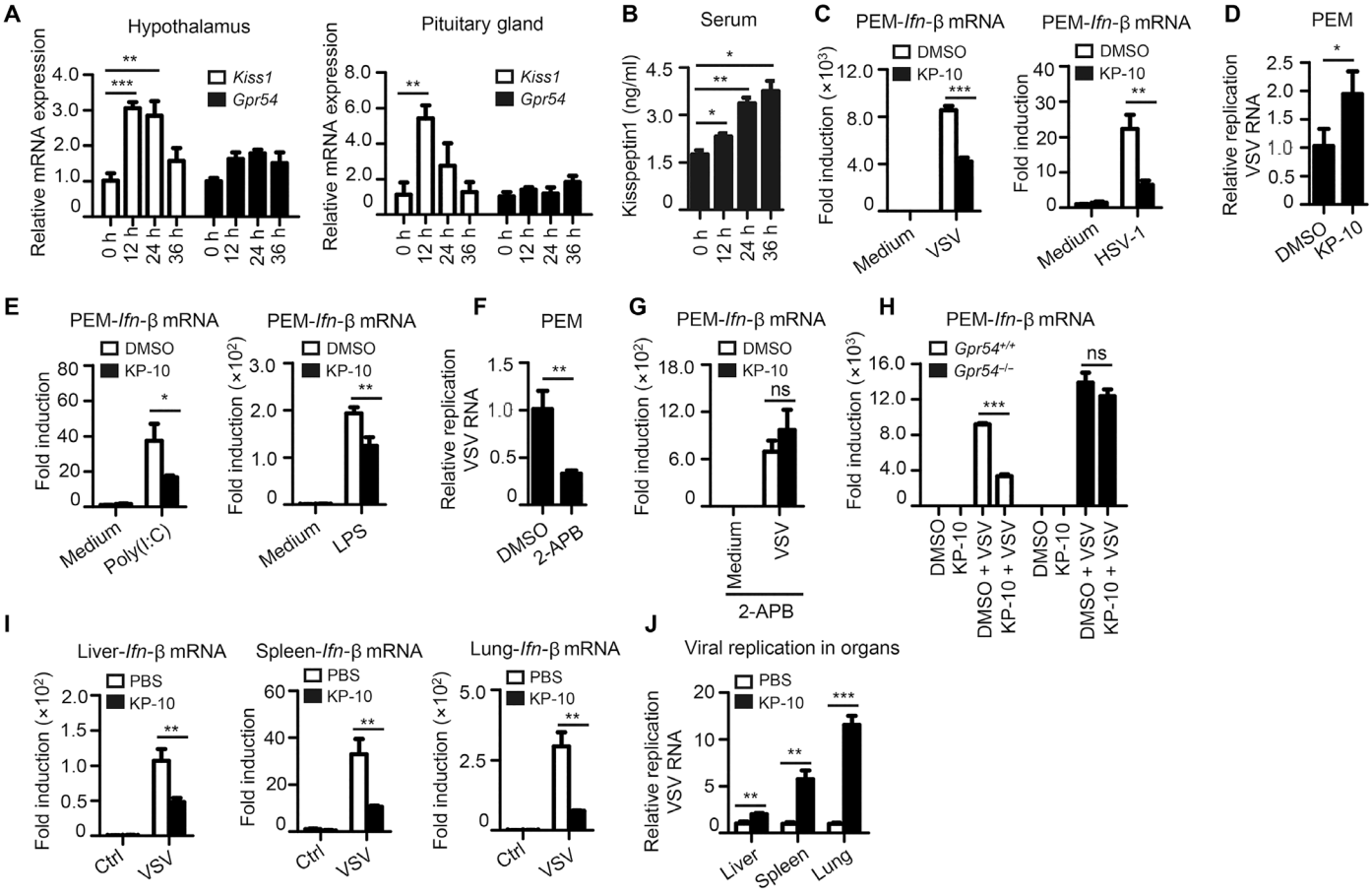

Fig. 3. Kisspeptin constrains virus-induced IFN-β production. (**A**) qPCR analysis of *Kiss1* and *Gpr54* expression in the hypothalamus or pituitary gland from mice infected with VSV (1×10^8 PFU per mouse) intraperitoneally for the indicated times. (**B**) ELISA of kisspeptin1 levels in sera from mice in (A). (**C**) qPCR analysis of *Ifn*-β expression in PEMs pretreated with KP-10 (1 μM) for 6 hours and then infected with VSV (MOI, 1) or HSV-1 (MOI, 1) for 8 hours. DMSO, dimethyl sulfoxide. (**D**) qPCR analysis of VSV RNA replicates in (C) (left panel). (**E**) qPCR analysis of *Ifn*-β expression in PEMs pretreated with KP-10 (1 μM) for 6 hours and then stimulated with poly(I:C) (10 μg/ml) or LPS (100 ng/ml) for 4 hours. (**F**) qPCR analysis of VSV RNA replicates in PEMs pretreated with 2-APB (100 μM) for 1 hour and then infected with VSV (MOI, 1) for 8 hours. (**G**) qPCR analysis of *Ifn*-β expression in PEMs pretreated with 2-APB (100 μM) for 1 hour before treatment with KP-10 (1 μM) for 6 hours and then infected with VSV (MOI, 1) for 8 hours. (**H**) qPCR analysis of *Ifn*-β expression in $Gpr54^{+/+}$ and $Gpr54^{-/-}$ PEMs pretreated with KP-10 (1 μM) for 6 hours and then infected with VSV (MOI, 1) for 8 hours. (**I**) qPCR analysis of *Ifn*-β expression in the liver, spleen, and lung from mice injected with KP-10 (50 μl of 1 mM KP-10) and VSV (1×10^8 PFU per mouse) for 12 hours and then treated with the same dosage of KP-10 again for 12 hours. (**J**) qPCR analysis of VSV RNA replicates in organs from mice in (I). *GAPDH* was used as an internal control for qPCR. Data are representative of three independent experiments (mean ± SD). $^*P < 0.05$, $^{**}P < 0.01$, $^{***}P < 0.001$. ns, not significant.

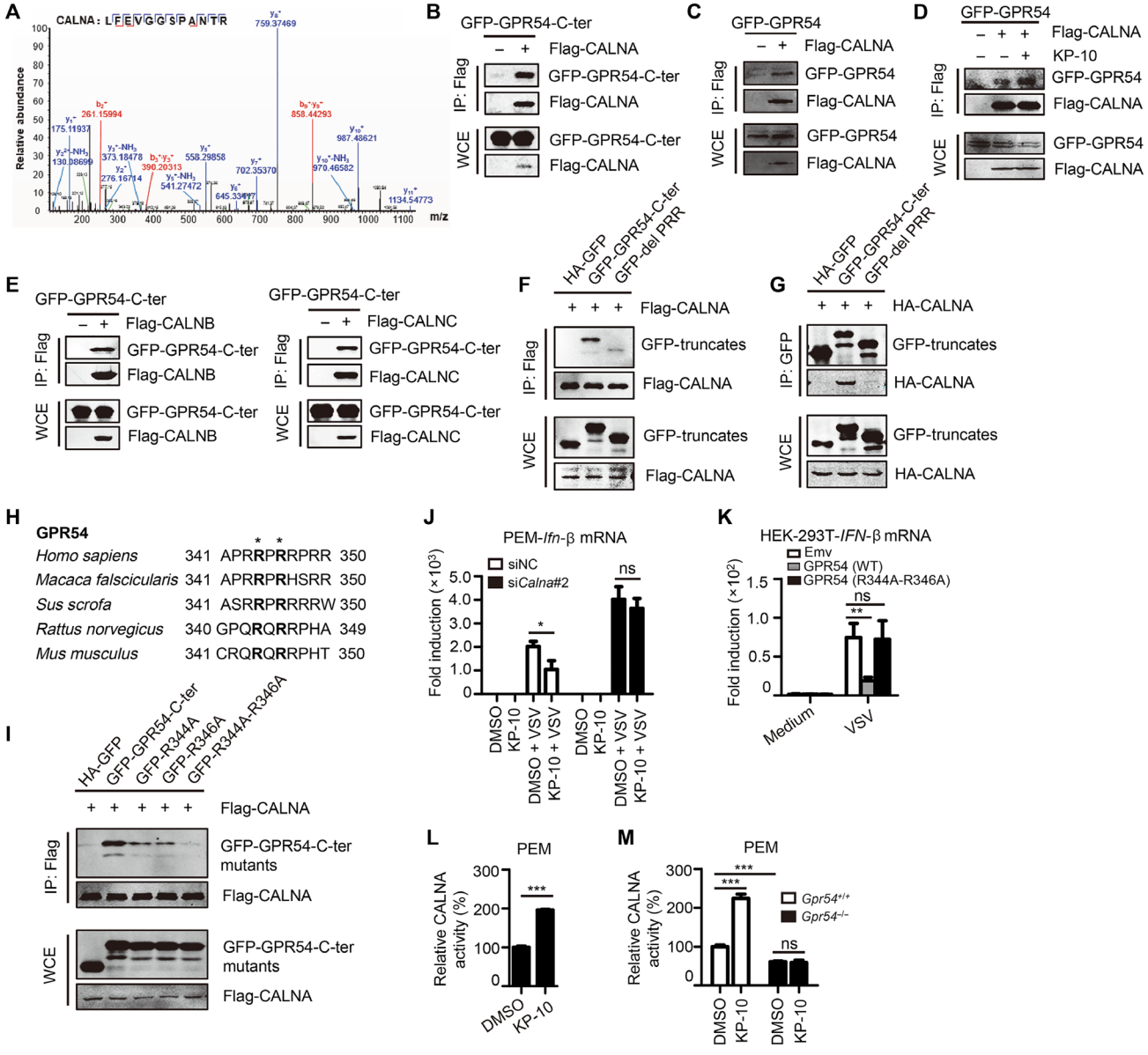

Fig. 4. Calcineurin mediates GPR54-dependent reduction of IFN-I. (**A**) HEK-293T cells were transfected with GFP-GPR54-C-ter (GFP-tagged C terminus of GPR54) for 36 hours, then GFP-GPR54-C-ter was immunoprecipitated with GFP antibody, and binding proteins were analyzed by MS. (**B**) HEK-293T cells were transfected with plasmids encoding GFP-GPR54-C-ter and Flag-CALNA for 28 hours. The supernatants of cell lysates were immunoprecipitated using M2 beads and then immunoblotted with antibodies to GFP or Flag tags. WCE, whole-cell extracts. (**C**) HEK-293T cells were transfected with plasmids encoding GFP-GPR54 and Flag-CALNA for 28 hours. The supernatants of cell lysates were immunoprecipitated using M2 beads and then immunoblotted with antibodies to GFP or Flag tags. (**D**) HEK-293T cells were transfected with plasmids encoding GFP-GPR54 and Flag-CALNA for 28 hours. The transfected cells were stimulated with KP-10 (1 μM) for 6 hours. The supernatants of cell lysates were immunoprecipitated using M2 beads and then immunoblotted with antibodies to GFP or Flag tags. (**E**) GFP-GPR54-C-ter was cotransfected with Flag-CALNB or Flag-CALNC into HEK-293T cells for 28 hours. The supernatants of cell lysates were immunoprecipitated using M2 beads and then immunoblotted with antibodies to GFP or Flag tags. (**F**) Flag-CALNA was cotransfected with GFP-GPR54-C-ter or GFP-GPR54-C-ter PRR repeats deleted (GFP-GPR54-C-ter-delPRR) into HEK-293T cells for 28 hours. The supernatants of cell lysates were immunoprecipitated using M2 beads and then immunoblotted with antibodies to GFP or Flag tags. (**G**) hemagglutinin (HA)–CALNA was cotransfected with GFP-GPR54-C-ter or GFP-GPR54-C-ter-delPRR into HEK-293T cells for 28 hours. The supernatants of cell lysates were immunoprecipitated using a GFP antibody and then immunoblotted with antibodies to HA or GFP tags. (**H**) Sequence analysis of the PRR repeats of GPR54 indicates that Arg^{344} and Arg^{346} (in bold) are conserved among species. (**I**) Flag-CALNA was cotransfected with GFP-GPR54-C-ter or GFP-GPR54-C-ter Arg^{344} and Arg^{346} mutants (arginine mutated to alanine) into HEK-293T cells for 28 hours. The supernatants of cell lysates were immunoprecipitated using M2 beads and then immunoblotted with antibodies to GFP or Flag tags. (**J**) qPCR analysis of *Ifn*-β expression in PEMs transfected with *Calna* siRNA for 48 hours before stimulated with KP-10 (1 μM) for 6 hours and then infected with VSV (MOI, 1) for 8 hours. (**K**) qPCR analysis of *IFN*-β expression in GFP-*GPR54*– or GFP-GPR54-R344A-R346A–overexpressing HEK-293T cells infected with VSV (MOI, 1) for 12 hours. WT, wild type. (**L** and **M**) $Gpr54^{+/+}$ and $Gpr54^{-/-}$ PEMs were pretreated with KP-10 (1 μM) for 6 hours, and the supernatants of cell lysates were immunoprecipitated using a CALNA antibody. The purified protein was used to measure CALNA activity by the standard pNpp method. *GAPDH* was used as an internal control for qPCR. Data are representative of three independent experiments (mean ± SD). $^{*}P < 0.05$, $^{**}P < 0.01$, $^{***}P < 0.001$.

replication was markedly restricted (Fig. 3F). Furthermore, the KP-10–induced reduction in *Ifn*-β production was eliminated by 2-APB, suggesting that the function of KP-10 is Ca^{2+}-dependent (Fig. 3G). Meanwhile, the ability of KP-10 to inhibit *Ifn*-β production also disappeared in *Gpr54*-deficient PEMs, which confirmed the specific activation of GPR54 signaling by KP-10 (Fig. 3H). Thus, kisspeptin restricts virus-induced IFN-I production in a Ca^{2+}-dependent manner. Notably, the expression of *Ifn*-β was significantly reduced in organs of KP-10–challenged mice compared with control mice (Fig. 3I). Accordingly, the replication of VSV in the organs of KP-10–challenged mice was increased obviously (Fig. 3J). Together, our data suggest that, although the virus-induced expression of kisspeptin mainly occurs in the neuroendocrine system, kisspeptin appears to function in peripheral macrophages to constrain antiviral innate immune response.

Calcineurin mediated GPR54-dependent reduction of IFN-I

It has been reported that there are several overlapping proline-arginine-arginine (PRR) repeats located within the intracellular domain of GPR54, which could be involved in intracellular signal transduction through binding downstream signaling molecules (*29*). So, we investigated the intracellular binding partners of GPR54 through mass spectrometry (MS) to explore the potential mechanism by which GPR54 regulated IFN-I. We found that the serine/threonine-protein phosphatase 2B catalytic subunit α isoform (CALNA) could bind with the C terminus of GPR54 (amino acids 328 to 398; Fig. 4A). Next, we further confirmed that the exogenous C-terminal (C-ter) cytoplasmic domain of GPR54 (Fig. 4B) and full-length GPR54 (Fig. 4C) both efficiently bound to exogenous CALNA by co-immunoprecipitation (CO-IP), and this interaction could be facilitated by KP-10, implying a key role of kisspeptin in the interaction between GPR54 and CALNA (Fig. 4D). Similarly, the other two calcineurin catalytic subunits β and γ (CALNB and CALNC) could also bind with the C terminus of GPR54 (Fig. 4E). These data indicate that calcineurin is a binding partner of GPR54.

To confirm whether PRR repeats are the specific binding sites in GPR54, we constructed GPR54 deletion mutants lacking the PRR repeats for CO-IP assay. As shown in Fig. 4 (F and G), CALNA binding was almost abolished in PRR repeats–deleted GPR54. Surprisingly, homology analysis of PRR repeats in GPR54 from different species indicates that only Arg^{344} and Arg^{346} (in bold) are conserved (Fig. 4H) (*30*). So, we speculated that Arg^{344} and Arg^{346} may be the key amino acids involved in interaction between GPR54 and CALNA. Accordingly, when we mutated these two arginines into alanines separately or together, the binding with CALNA was reduced significantly (Fig. 4I). To study whether calcineurin mediated kisspeptin/GPR54 regulation of IFN-I, we constructed CALNA knockdown PEMs using three different small interfering RNA (siRNA) sequences (fig. S3, A and B). We found that *Ifn*-β production was enhanced and that KP-10–mediated restriction of *Ifn*-β was eliminated in CALNA knockdown PEMs (Fig. 4J). In addition, overexpression of the GPR54 (R344A and R346A) mutant could not inhibit VSV-induced *IFN*-β expression (Fig. 4K). These data suggest that kisspeptin/GPR54 reduced IFN-β production in a CALNA-dependent manner.

Next, we sought to determine how CALNA is regulated by kisspeptin/GPR54. Our data show that the stability of CALNA was not influenced by KP-10 or GPR54 (fig. S3, C and D). Considering that kisspeptin/GPR54 restricts IFN-I production in a Ca^{2+}-dependent

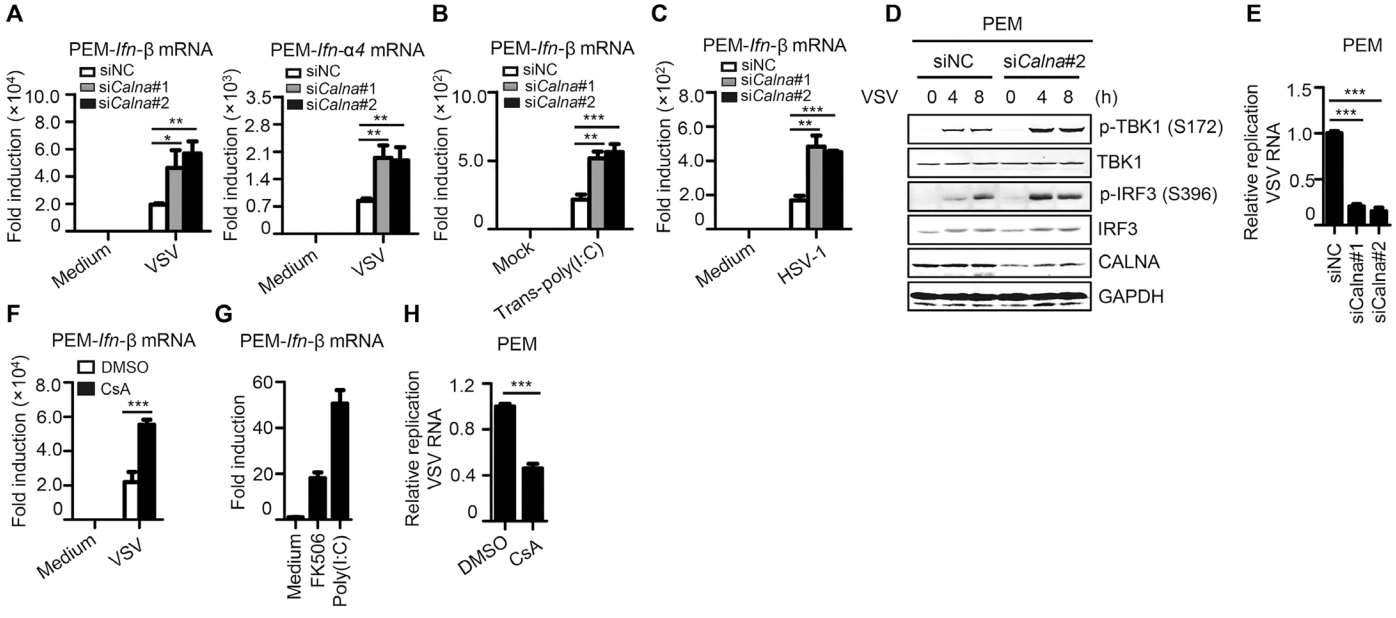

Fig. 5. Calcineurin negatively regulates IFN-I signaling. (**A**) qPCR analysis of *Ifn*-β and *Ifn*-*α4* expression in PEMs transfected with *Calna* siRNA for 48 hours and then infected with VSV (MOI, 1) for 8 hours. (**B**) qPCR analysis of *Ifn*-β expression in PEMs transfected with *Calna* siRNA for 48 hours and then transfected with poly(I:C) (1 μg/ml) for 4 hours. (**C**) qPCR analysis of *Ifn*-β expression in PEMs transfected with *Calna* siRNA for 48 hours and then infected with HSV-1 (MOI, 10) for 8 hours. (**D**) Immunoblot analysis of phosphorylated TBK1 and IRF3 or total proteins in lysates of PEMs transfected with *Calna* siRNA for 48 hours and then infected with VSV (MOI, 1) for the indicated times. (**E**) qPCR analysis of VSV RNA replicates in (A). (**F**) qPCR analysis of *Ifn*-β expression in PEMs pretreated with CsA (10 μg/ml) for 1 hour and then infected with VSV (MOI, 1) for 8 hours. (**G**) qPCR analysis of *Ifn*-β expression in PEMs treated with FK506 (10 μg/ml) or poly(I:C) (10 μg/ml) for 4 hours. (**H**) qPCR analysis of VSV RNA replicates in (F). *GAPDH* was used as an internal control for qPCR. Data are representative of three independent experiments (mean ± SD). **P* < 0.05, ***P* < 0.01, ****P* < 0.001.

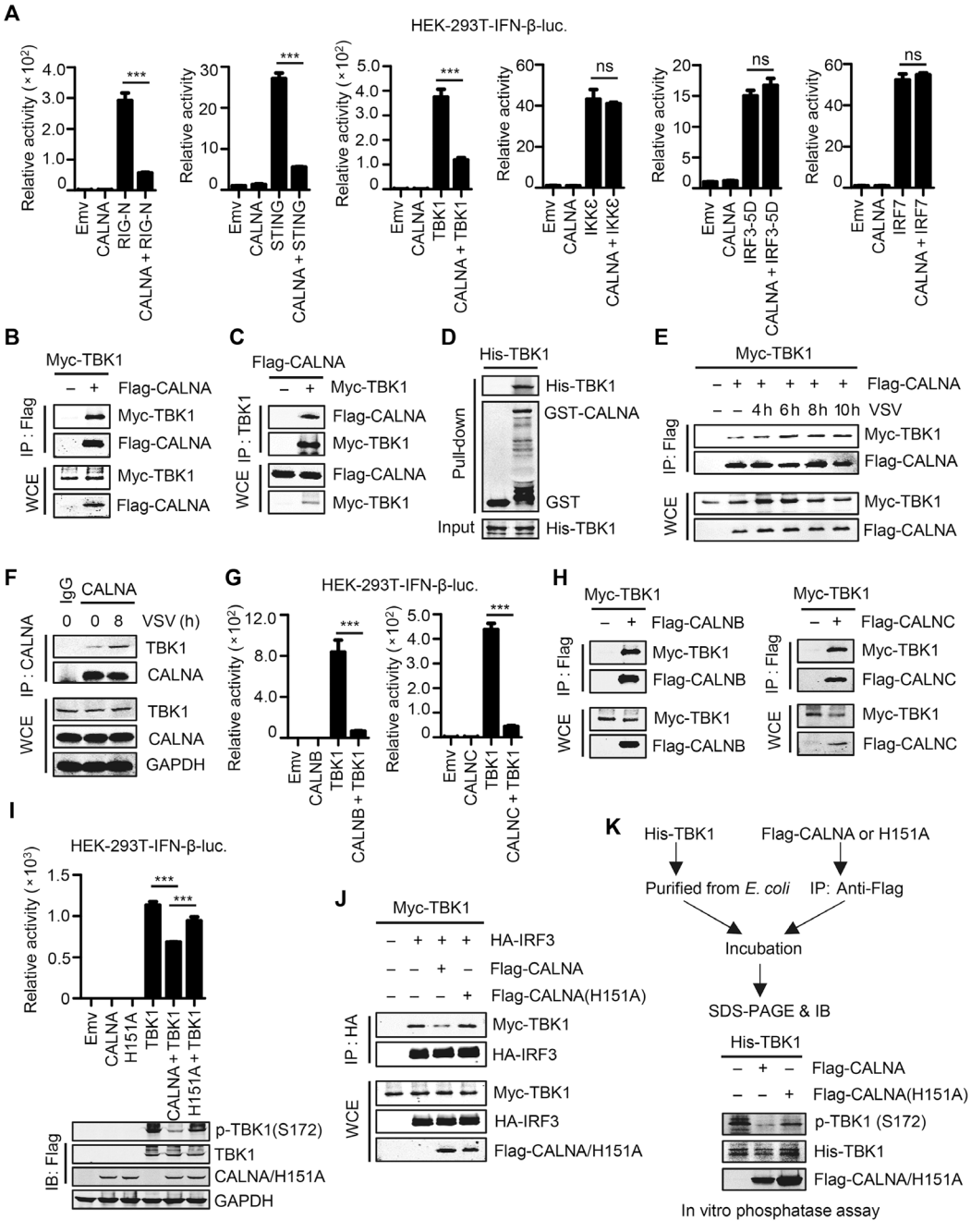

Fig. 6. Calcineurin targets and deactivates TBK1 through dephosphorylation. (**A**) Flag-CALNA was cotransfected with RIG-I(N) (RIG-N), STING, TBK1, IKKε, IRF3-5D, IRF7, or Emvs, together with IFN-β luciferase reporter, into HEK-293T cells for 28 hours. IFN-β luciferase activity was detected and normalized to *Renilla* luciferase activity. (**B** and **C**) HEK-293T cells were transfected with plasmids encoding Myc-TBK1 and Flag-CALNA for 28 hours. The supernatants of cell lysates were immunoprecipitated using M2 beads (B) or a TBK1 antibody (C) and then immunoblotted with antibodies to TBK1 or Flag tag. (**D**) Purified GST-CALNA protein was incubated with purified His-TBK1. After GST pull-down assay, the proteins were immunoblotted with antibodies to TBK1 or GST tag. (**E**) HEK-293T cells transfected with Myc-TBK1 and Flag-CALNA for 28 hours were infected with VSV (MOI, 1) for the indicated times. The supernatants of cell lysates were immunoprecipitated using M2 beads and then immunoblotted with antibodies to TBK1 or Flag tag. (**F**) PEMs were infected with VSV (MOI, 1) for 8 hours. The supernatants of cell lysates were immunoprecipitated using a CALNA antibody and then immunoblotted with antibodies to CALNA or TBK1. (**G**) Flag-TBK1 was cotransfected with Flag-CALNB or Flag-CALNC, together with the IFN-β luciferase reporter, into HEK-293T cells for 28 hours. IFN-β luciferase activity was detected and normalized to *Renilla* luciferase activity. (**H**) Myc-TBK1 was cotransfected with Flag-CALNB or Flag-CALNC for 28 hours. The supernatants of cell lysates were immunoprecipitated using M2 beads and then immunoblotted with antibodies to TBK1 or Flag tag. (**I**) Flag-TBK1 was cotransfected with Flag-CALNA, Flag-CALNA (H151A) or Emvs, together with IFN-β luciferase reporter, into HEK-293T cells for 28 hours. IFN-β luciferase activity was detected and normalized to *Renilla* luciferase activity. IB, immunoblotting. (**J**) HEK-293T cells were transfected with the indicated plasmids. The supernatants of cell lysates were immunoprecipitated using HA beads and then immunoblotted with the indicated antibodies. (**K**) Purified His-TBK1 from *Escherichia coli* was incubated with Flag-CALNA or Flag-CALNA (H151A), which had been expressed in HEK-293T cells. In vitro phosphatase assays were performed, and then, proteins were immunoblotted with the indicated antibodies. Data are representative of three independent experiments (mean ± SD). ***$P < 0.001$.

manner and that calcineurin is a Ca^{2+}-dependent phosphatase (*31*), we speculated that the activity of calcineurin may be regulated by kisspeptin/GPR54 signaling. Thus, we treated the wild-type or *Gpr54*-deficient PEMs with KP-10 and found that the activity of CALNA was enhanced by KP-10 in a GPR54-dependent manner (Fig. 4, L and M). Previous studies have shown that PP2A binds with GPR54 (*29*), and PP2A negatively regulates the expression of IFN-β (*32*). Although we confirmed these findings, KP-10–reduced *Ifn*-β production remained in PP2A knockdown cells, which implied that PP2A is not involved in GPR54-mediated regulation of IFN-I (fig. S3, E to G). Together, these results suggest that kisspeptin and GPR54 restrict IFN-I production through regulating calcineurin phosphatase activity.

Calcineurin negatively regulates IFN-I signaling

To further evaluate the negative regulation of IFN-I production by calcineurin, we activated IFN-I production through VSV infection (Fig. 5A), poly(I:C) transfection (Fig. 5B), or HSV-1 infection (Fig. 5C) and found that the expression of IFN-I was enhanced in CALNA knockdown PEMs. Similar data were also observed in poly(I:C)- or LPS-stimulated cells (fig. S4A). Consequently, the VSV-induced (Fig. 5D), poly(I:C)-induced, and LPS-induced (fig. S4B) phosphorylation of both TBK1 (Ser^{172}) and IRF3 (Ser^{396}) were significantly increased in CALNA knockdown PEMs. At the same time, we found that VSV replication in CALNA knockdown cells was decreased significantly (Fig. 5E). In addition, the production of *Ifn*-β was enhanced following treatment with cyclosporin A (CsA; Fig. 5F) and tacrolimus (FK506) (Fig. 5G), which are both specific inhibitors of CALNA. Accordingly, the VSV replication in PEMs was reduced by CsA (Fig. 5H). Therefore, calcineurin is important in negative regulation of IFN-I signaling.

Calcineurin deactivates TBK1 through dephosphorylation

To further explore the mechanism of calcineurin regulation of IFN-I production, we used an IFN-β and IRF3 luciferase reporter to test which components are involved in calcineurin-mediated regulation. We found that the activity of IFN-β luciferase were inhibited by CALNA in RIG-I(N)-, STING (stimulator of IFN gene)–, and TBK1-cotransfected HEK-293T cells but not in inhibitor of nuclear factor κB kinase ε (IKKε)–cotransfected, IRF3-5D–cotransfected (a constitutively active form of IRF3), or IRF7-cotransfected cells (Fig. 6A). Similar results were also observed in IRF-3 luciferase reporter assay (fig. S5A). These results suggest that CALNA may act on TBK1-mediated IFN-I production.

Next, we examined whether CALNA could bind to TBK1. Our data show that CALNA co-immunoprecipitated with TBK1 (Fig. 6, B and C). Furthermore, prokaryotically expressed CALNA and TBK1 also directly interacted in a glutathione *S*-transferase (GST) pull-down assay (Fig. 6D). VSV infection increased the interaction between both exogenous and endogenous CALNA and TBK1 (Fig. 6, E and F). Similarly, the other two calcineurin catalytic subunits β and γ (CALNB and CALNC) also decreased the activity of TBK1-induced IFN-β luciferase and also bound to TBK1 (Fig. 6, G and H). Although the interaction between CALNA and TBK1 was enhanced by VSV infection, KP-10 had no effect on the interaction between TBK1 and CALNA (fig. S5, B and C). To further determine which domain of TBK1 is responsible for its interaction with calcineurin, we constructed several deletion constructs of TBK1 (fig. S5D). CO-IP (fig. S5E) and GST pull-down (fig. S5F) assays revealed that all three domains of TBK1 interacted with CALNA. These data together indicate that CALNA binds to TBK1 directly.

As calcineurin-mediated physiological effects occur mainly through the dephosphorylation of its substrates, and mutating histidine 151 inactivates CALNA phosphatase activity (*33*), we constructed CALNA (H151A) plasmids and examined whether TBK1 is dephosphorylated by calcineurin. Our data demonstrated that CALNA (H151A) barely inhibited the activity of TBK1-induced IFN-β luciferase (Fig. 6I). Consistently, the recruitment of IRF3 by TBK1 was reduced by CALNA but was not influenced by CALNA (H151A; Fig. 6J). Similar data were also observed in an in vitro dephosphorylation assay, suggesting that CALNA phosphatase activity is crucial in restricting TBK1 phosphorylation at Ser^{172}, which is important in TBK1-mediated IFN-I signaling (Fig. 6K). Although GSK3β could facilitate TBK1 phosphorylation at Ser^{172} in a kinase-independent manner (*5*), an interaction between CALNA and GSK3β was not observed in a CO-IP assay (fig. S5G). Also, in CALNA knockdown PEMs, LPS-induced TBK1 phosphorylation was increased obviously, but the phosphorylation and stability of GSK3β were unchanged (fig. S5H), suggesting that CALNA-reduced TBK1 phosphorylation is independent of GSK3β. Furthermore, although IRF3 could be dephosphorylated by both PP1 (*34*) and PP2A (*32*), CALNA could not bind with IRF3, although it has structural similarities with PP1 and PP2A (fig. S5I). When we cotransfected HEK-293T cells with TBK1, the C terminus of GPR54, and CALNA, CALNB, or CALNC, both TBK1 and the C terminus of GPR54 could bind with calcineurin (fig. S5J). In addition, overexpression of GPR54 only inhibited phosphorylation of TBK1 (Ser^{172}) but not affected phosphorylation of IKKε (Ser^{172}) or phosphorylation of IRF7 (Ser^{477}), which are both important proteins in IFN-I signaling pathways (fig. S5K). Consistent with this observation, CALNA could not bind to IKKε or IRF7 in GST pull-down assays (fig. S5L). Collectively, these results suggest that the kisspeptin/GPR54/calcineurin axis could reduce virus-induced IFN-I production through specifically binding and dephosphorylating TBK1.

DISCUSSION

Here, we uncover a novel regulatory loop centered on kisspeptin and GPR54 that functions to limit the intensity of antiviral innate immune response (fig. S6). In this loop, viral infection induces kisspeptin secretion from kisspeptin-containing tissues. Kisspeptin activating GPR54 in peripheral immune cells induces binding of calcineurin to the GPR54 cytoplasmic domain and results in calcineurin activation in a Ca^{2+}-dependent manner. Calcineurin, in turn, dephosphorylates TBK1 and inhibits IFN-I production. Thus, kisspeptin/GPR54 signaling forms a negative feedback loop to limit TBK1 signaling and IFN-I expression, which may constitute a virus-exploited immune evasion pathway during infection.

While IFN-I is protective in acute viral infection, it can have either protective or deleterious roles in bacterial infection and autoimmune diseases (*3*). Thus, the IFN-I response must be tightly regulated by host, pathogen, and environmental factors to maintain immune homeostasis. As the most crucial kinase in IFN-I signaling, TBK1 not only phosphorylates the downstream transcription factors IRF3 and IRF7 to induce inflammatory cytokines and IFN-I production but also activates a series of adaptor proteins such as MAVS (mitochondrial antiviral signaling protein), STING, and TRIF [toll/interleukin-1 receptor (TIR) domain-containing adaptor inducing IFN-β], which are all crucial in the antiviral innate immune response (*35*). Here, we found that the kisspeptin/GPR54/calcineurin axis targets and dephosphorylates TBK1 to negatively regulate TBK1-mediated

IFN-I production and antiviral immunity. This is slightly different from the work of Kang *et al.* (*36*), who reported that calcineurin negatively regulates inflammatory response through inhibiting MYD88 (myeloid differentiation factor 88), TRIF, and a subset of TLRs in macrophages. We cannot rule out a contribution of these pathways downstream of calcineurin in regulating macrophage antiviral IFN response. However, Liu *et al.* (*35*) found that TBK1 could phosphorylate TRIF to induce IRF3 activation and IFN-I production. Thus, whether inhibition of TRIF by calcineurin is mediated by TBK1 in regulation of IFN-I still needs to be further investigated. At any rate, our findings highlight TBK1 as a crucial target of the kisspeptin/GPR54/calcineurin axis in regulating antiviral innate immune response.

Several GPR54 inactivating mutations have been reported in patients displaying hypogonadotropic hypogonadism (*37*). Also, a patient with GPR54-activating mutation (Arg^{386} Pro) was found with central precocious puberty (*38*). While immune sequelae of GPR54 inactivating or activating mutations have not been reported to date, kisspeptin is highly produced by the placenta and contributes to the formation of immune tolerance to antigens of the fetoplacental unit during pregnancy through regulation of adaptive regulatory T and T helper 17 cells, as well as IDO (indolamin 2,3 dioxygenase) expression by monocytes (*27*). In light of our findings, we would predict immune sequelae in humans bearing GPR54 mutations. Thus, it would be intriguing to examine the susceptibility or immune injury of bodies in these GPR54-activated or GPR54-inactivated patients during viral infection.

In addition to our findings here, calcineurin is a novel phosphatase involved in TBK1-mediated IFN-I production, and PPM1A (*9*, *10*), PPM1B (*11*), and PP4 (*12*) all bind to and dephosphorylate TBK1. Unique among these phosphatases, the activity of calcineurin is Ca^{2+}-dependent and specifically regulated by kisspeptin/GPR54-associated GPCR signaling during viral infection. The Ca^{2+}-dependent kinase calcium/calmodulin-dependent protein kinase II was activated by TLR-induced Ca^{2+} and found to facilitate IFN-I production through phosphorylating TAK1 (transforming growth factor β–activated kinase 1) and IRF3 (*39*), suggesting that the role of Ca^{2+} in antiviral innate immune response is complicated. We speculate that the contradictory role may be due to different sources of Ca^{2+} (TLRs or GPCRs). Although TLRs and some viruses could induce release of Ca^{2+}, Ca^{2+} was not detected after VSV infection (*40*), which indicates that calcineurin activity may be independent of virus-induced Ca^{2+}. At any rate, our data provide new evidence about how Ca^{2+} works as a switch in regulation of antiviral innate immune response through balancing the activities of kinases and phosphatases.

The calcineurin-specific inhibitor CsA has been widely used as an immunosuppressive agent, in preventing rejection following solid organ transplantation and treating graft-versus-host disease following bone marrow transplant, as well as in autoimmune diseases such as psoriasis, rheumatoid arthritis, and nephrotic syndrome (*41*). However, CsA was found to inhibit the replication of both hepatitis C virus (HCV) (*42*) and HIV (*43*). Furthermore, a series of studies demonstrated that CsA restricts the replication of rotavirus (*44*) and HCV (*45*) through up-regulating IFN-I production. Similarly, when we inhibited the activity of calcineurin with CsA, the virus-induced IFN-β increased significantly, which may partially explain why CsA could be used in treating viral diseases. Thus, viral infectious diseases could be a new indication for CsA, repurposing the "old" immunosuppressive agent into novel applications. It is well known that virus-stimulated severe inflammation could be a main reason for tissue damage, serious respiratory problems, ultimately multiple organ failure, and even death. Thus, treating patients with CsA for viral infectious diseases may reduce overactive inflammation and virus replication, which could have synergistic effects in treating viral diseases.

Together, we identified kisspeptin as a novel virus-induced neuropeptide hormone that activates GPR54 to negatively regulate IFN-I production and control the intensity of antiviral innate immune response. As the most important drug targets, about 50% of current therapeutic drugs on the market target GPCRs directly or indirectly (*16*). Thus, our study demonstrated a new avenue to develop drugs targeting GPCRs to treat viral diseases, by inhibiting the kisspeptin/GPR54/calcineurin axis to enhance antiviral response.

MATERIALS AND METHODS

Chemicals, reagents, and antibodies

Dulbecco's modified Eagle's medium (DMEM), RPMI 1640, penicillin-streptomycin, and Lipofectamine 2000 were obtained from Invitrogen Life Technologies. Fetal bovine serum (FBS) was purchased from Gibco. TRIzol reagent and PrimeScript RT Master Mix were acquired from Takara. SYBR Green PCR Master Mix was purchased from Yeasen. CsA and tacrolimus (FK506) (calcineurin inhibitors) were purchased from Selleck. Poly(I:C) (TLR3 ligand), R848 (TLR7/8 ligand), and ODN2395 (TLR9 ligand) were obtained from Invivogen. LPS and recombinant mouse IFN-β protein were purchased from Sigma-Aldrich and Sino Biological, respectively. KP-10 was provided by H. Zhang (East China Normal University). A dual-luciferase assay reagent was purchased from Promega. The antibodies used in this research are listed as follows: Flag (Biogot Technology), HA (Biogot Technology), GAPDH (Biogot Technology), GFP (Abmart), His (Proteintech), GST (Abcam), TBK1 (Cell Signaling Technology), p-TBK1 (Cell Signaling Technology), IRF3 (Cell Signaling Technology), p-IRF3 (Cell Signaling Technology), p-IKKε (Cell Signaling Technology), p-IRF7 (Cell Signaling Technology), GPR54 (Santa Cruz Biotechnology), Pan-calcineurin A (Cell Signaling Technology), GSK3α/β (Cell Signaling Technology), and p-GSK3α/β (Cell Signaling Technology). M2 beads (Sigma-Aldrich), HA beads (Abmart), Protein A/G beads (Abmart), and Glutathione Sepharose 4B (GE Healthcare Life Sciences) were purchased.

Cell culture

HEK-293T, HeLa, Raw264.7, and Vero were purchased from the American Type Culture Collection and cultured in DMEM supplemented with 10% FBS and 1% penicillin-streptomycin. PEMs and BMMs were prepared, as described previously (*46*).

Plasmids and transfection

Flag-RIG-I(N), Flag-MAVS, Flag-TBK1, Myc-TBK1, STING-HA, HA-GSK3β, Flag-PPP2CA, Flag-PPP2CB, Flag-CALNA, Flag-CALNB, Flag-CALNC, IFN-β reporter, and *Renilla* plasmids were gifts from P. Wang (Tongji University). Flag-IRF3-5D mutant and Flag-IRF7 plasmids were provided by D. Xie (Institute for Nutritional Sciences, Shanghai Institutes for Biological Sciences, Chinese Academy of Sciences). IRF3 reporter plasmids were provided by X. Wang (Zhejiang University). HA-CALNA and HA-IRF3 were purchased from Biogot Technology. GFP-GPR54 plasmid was obtained from GeneCopoeia, and GFP-GPR54-R344A-R346A was constructed into the same vector by point mutation. Flag-CALNA (H151A) and Flag-IKKε were cloned

into Flag-pcDNA3.1. GFP-GPR54-C-ter (328-398aa), GFP-GPR54-C-ter-delPRR (358-398aa), GFP-GPR54-C-ter-R344A, GFP-GPR54-C-ter-R346A, GFP-GPR54-C-ter-R344A-R346A, GFP-TBK1, or GFP-TBK1 truncates were cloned into GFP-pcDNA3.1. His-TBK1, His-IRF3, His-IKKε, His-IRF7, and His-CALNA were cloned into pet28a. GST-CALNA, GST-TBK1, and GST-TBK1 truncates were cloned into pGEX-4T-2. All plasmids and mutants were constructed by standard PCR techniques. All constructs were sequenced. Transfection was performed using the calcium phosphate–DNA coprecipitation method for HEK-293T cells and Lipofectamine 2000 (Invitrogen) for HeLa cells, according to the manufacturer's protocols. Cells transfected with the same amount of Emv were used as control and normalized for transfection efficiency.

Luciferase reporter assay

HEK-293T cells were transfected with IFN-β or IRF3 reporter plasmids together with *Renilla* plasmids and other described gene constructs for 28 hours. The cells were lysed and measured for luciferase activity with a dual-luciferase assay, according to the manufacturer's instructions (Promega).

RNA interference

PEMs were seeded into 12-well plates at 1.5×10^6 cells per well overnight and transfected with 50 nM siRNA using transexcellent-siRNA [from Y. Cheng (East China Normal University)] for 48 hours, according to the manufacturer's protocol. The PEMs transfected with the same amount of universal nontargeting siRNA were used as a negative control (siNC). Mouse *Ppp2ca*-specific siRNA oligos (SR409313) and *Calna*-specific siRNA oligos (SR416619) were purchased from OriGene.

Real-time qPCR

Total RNA were extracted with a TRIzol reagent (Takara) and subjected to reverse transcription with PrimeScript RT Master Mix (Takara). The reverse transcription products were amplified by real-time qPCR using SYBR Green PCR Master Mix (Yeasen). Primers for each cytokine and gene are listed in table S1.

Enzyme-linked immunosorbent assay

Human or mouse IFN-β in cell culture supernatants or sera from virus-infected mice were measured by human IFN-β ELISA kits (Shanghai Yinggongshiye Inc.) or mouse IFN-β ELISA kits (BioLegend) according to the manufacturer's instructions. kisspeptin1 levels in sera from virus-infected mice were measured by a mouse kisspeptin1 ELISA kit (MyBioSource) according to the manufacturer's instructions.

Immunoprecipitation analysis and immunoblot analysis

Transfected cells were lysed in lysis buffer [50 mM tris-HCl (pH 7.4), 150 mM NaCl, 10% glycerol, 1 mM EDTA, and 0.5% NP-40] containing 1 mM phenylmethylsulfonyl fluoride, 1 mM NaF, and 1 mM Na_3VO_4. The supernatants of cell lysates were immunoprecipitated with 10 μl of M2 beads/HA beads for 3 hours at 4°C. To detect endogenous protein interactions, PEMs were infected with VSV (MOI, 1) for the indicated times, and cells were lysed in Cytobuster Protein Extraction Buffer (Novagen) and then incubated with the indicated antibody and 20 μl of protein A/G beads for 6 hours at 4°C. After extensive washing, beads were heated at 100°C for 15 min, separated by SDS–polyacrylamide gel electrophoresis (PAGE), transferred to nitrocellulose membranes, and blocked with 5% bovine serum albumin (BSA), followed by immunoblotting with the indicated antibodies. The immunoreactive bands were visualized by the Odyssey system (LI-COR Biosciences).

GST pull-down assay

GST and GST-fusion proteins were purified with Glutathione Sepharose 4B from *E. coli* for 2 hours. Then, the beads were washed three times and incubated with *E. coli* lysates that expressed His-tagged proteins at 4°C for 2 hours. Precipitates were extensively washed and subjected to SDS-PAGE.

Virus propagation

Indiana serotype of VSV and HSV-1 were provided by P. Wang (Tongji University). NDV-GFP virus and VSV-GFP virus were gifts from J. Han (Xiamen University) and A. Cimarelli (Ecole Normale Supérieure de Lyon), respectively. All viruses were propagated in a monolayer of Vero cells, and the titers were determined by standard plaque assays.

Mice

Gpr54-deficient mice (C57BL/6) were generated as previously described (*24*). Primers used for the identification of mutated mice are 5′-GCCTAAGTTTCTCTGGTGGAGGATG-3′ (wild-type), 5′-GTGGGATTAGATAAATGCCTGCTCT-3′ (knockout), and 5′-CGCGTACCTGCTGGATGTAGTTGAC-3′ (common). Age- and sex-matched mice were used for related experiments. All mice were bred in specific pathogen–free rooms. Animal procedures were approved by the Institutional Animal Ethics Committee of East China Normal University.

Lung histology

Lungs from control or VSV-infected mice were dissected, fixed in 4% paraformaldehyde, embedded into paraffin, sectioned, stained with hematoxylin and eosin, and examined by light microscopy for histologic changes.

KP-10 challenge in vivo

The in vivo KP-10 challenge was performed as previously described (*47*), with minor modifications. Briefly, adult mice were intraperitoneally injected with 50 μl of 1 mM KP-10 or 50 μl of phosphate-buffered saline (vehicle control) and given intraperitoneal infection of VSV (1×10^8 PFU per mouse) for 12 hours. Then, the mice were treated with the same dosage of KP-10 or phosphate-buffered saline again. Twelve hours later, mice were killed, and organs were collected to examine cytokines and VSV replication.

Immunofluorescence

HeLa and Raw264.7 cells were transfected with GFP-GPR54 for 28 hours, and the transfected cells were infected with VSV (MOI, 1) for the indicated times. Then, the cells were fixed in 4% paraformaldehyde. Next, the fixed cells were permeabilized using 0.1% Triton X-100 and stained for nucleic acids with 4′,6-diamidino-2-phenylindole (0.4 μg/ml). GFP-GPR54 localizations were observed under an LSM 510 Meta confocal system (Zeiss; original magnification, ×100).

Flow cytometry

$Gpr54^{+/+}$ and $Gpr54^{-/-}$ PEMs were infected with VSV-GFP (MOI, 0.01) for 12 hours, and VSV-GFP was measured by FACS (BD Biosciences) and analyzed using FlowJo software.

In vitro phosphatase assay

Flag-CALNA or Flag-CALNA (H151A) proteins were immunoprecipitated from cell lysates of HEK-293T cells transfected with plasmids encoding Flag-CALNA or Flag-CALNA (H151A), respectively. His-TBK1 protein was purified from *E. coli* and then subjected to in vitro phosphatase assay in phosphatase buffer [100 mM tris (pH 7.5), 100 mM NaCl, 0.4 mM $CaCl_2$, 200 nM calmodulin, BSA (100 μg/ml), 1 mM $MnCl_2$, and 0.5 mM dithiothreitol]. Reactions continued for 1 hour at 30°C and were stopped by the addition of 2× SDS loading buffer.

Calcineurin activity assay with pNpp

$Gpr54^{+/+}$ and $Gpr54^{-/-}$ PEMs were starved overnight and then treated with KP-10 (1 μM) for 6 hours. Endogenous CALNA was immunoprecipitated from cell lysates with immunoglobulin G or CALNA antibody, and its phosphatase activity was measured by the pNpp method as previously described (*48*).

MS analysis

In brief, HEK-293T cells were transfected with plasmids encoding GFP-GPR54-C-ter (GFP-tagged C terminus of GPR54) for 36 hours, the supernatants of cell lysates were immunoprecipitated using GFP antibody, and the binding proteins were analyzed by MS (Shanghai Wayen Biotechnologies Inc.). Binding partners of GFP-GPR54-C-ter identified by MS analysis are listed in table S2.

Statistical analysis

Kaplan-Meier curves present mouse survival rates. All data were analyzed by a Student's *t* test using Prism 5.0 (GraphPad Software). Except for the indicated mean ± SEM in the text, all values are shown as means ± SD. In all tests, *P* values less than 0.05 were considered to be statistically significant.

SUPPLEMENTARY MATERIALS

Supplementary material for this article is available at http://advances.sciencemag.org/cgi/content/full/4/8/eaas9784/DC1

Fig. S1. Related to Fig.1.
Fig. S2. Related to Fig.3.
Fig. S3. Related to Fig.4.
Fig. S4. Related to Fig.5.
Fig. S5. Related to Fig.6.
Fig. S6. Kisspeptin/GPR54/calcineurin axis–mediated TBK1 deactivation.
Table S1. The primer sequences for qPCR analysis.
Table S2. Binding partners of GFP-GPR54-C-ter identified by MS analysis.

REFERENCES AND NOTES

1. J. Wu, Z. J. Chen, Innate immune sensing and signaling of cytosolic nucleic acids. *Annu. Rev. Immunol.* **32**, 461–488 (2014).
2. W. M. Schneider, M. D. Chevillotte, C. M. Rice, Interferon-stimulated genes: A complex web of host defenses. *Annu. Rev. Immunol.* **32**, 513–545 (2014).
3. G. Trinchieri, Type I interferon: Friend or foe? *J. Exp. Med.* **207**, 2053–2063 (2010).
4. K. A. Fitzgerald, S. M. McWhirter, K. L. Faia, D. C. Rowe, E. Latz, D. T. Golenbock, A. J. Coyle, S.-M. Liao, T. Maniatis, IKKepsilon and TBK1 are essential components of the IRF3 signaling pathway. *Nat. Immunol.* **4**, 491–496 (2003).
5. C.-Q. Lei, B. Zhong, Y. Zhang, J. Zhang, S. Wang, H.-B. Shu, Glycogen synthase kinase 3β regulates IRF3 transcription factor-mediated antiviral response via activation of the kinase TBK1. *Immunity* **33**, 878–889 (2010).
6. S. Li, L. Wang, M. Berman, Y.-Y. Kong, M. E. Dorf, Mapping a dynamic innate immunity protein interaction network regulating type I interferon production. *Immunity* **35**, 426–440 (2011).
7. C. Wang, T. Chen, J. Zhang, M. Yang, N. Li, X. Xu, X. Cao, The E3 ubiquitin ligase Nrdp1 'preferentially' promotes TLR-mediated production of type I interferon. *Nat. Immunol.* **10**, 744–752 (2009).
8. G. Song, B. Liu, Z. Li, H. Wu, P. Wang, K. Zhao, G. Jiang, L. Zhang, C. Gao, E3 ubiquitin ligase RNF128 promotes innate antiviral immunity through K63-linked ubiquitination of TBK1. *Nat. Immunol.* **17**, 1342–1351 (2016).
9. Z. Li, G. Liu, L. Sun, Y. Teng, X. Guo, J. Jia, J. Sha, X. Yang, D. Chen, Q. Sun, PPM1A regulates antiviral signaling by antagonizing TBK1-mediated STING phosphorylation and aggregation. *PLOS Pathog.* **11**, e1004783 (2015).
10. W. W. Xiang, Q. Zhang, X. Lin, S. Wu, Y. Zhou, F. Meng, Y. Fan, T. Shen, M. Xiao, Z. Xia, J. Zou, X.-H. Feng, P. Xu, PPM1A silences cytosolic RNA sensing and antiviral defense through direct dephosphorylation of MAVS and TBK1. *Sci. Adv.* **2**, e1501889 (2016).
11. Y. Zhao, L. Liang, Y. Fan, S. Sun, L. An, Z. Shi, J. Cheng, W. Jia, W. Sun, Y. Mori-Akiyama, H. Zhang, S. Fu, J. Yang, PPM1B negatively regulates antiviral response via dephosphorylating TBK1. *Cell. Signal.* **24**, 2197–2204 (2012).
12. Z. Zhan, H. Cao, X. Xie, L. Yang, P. Zhang, Y. Chen, H. Fan, Z. Liu, X. Liu, Phosphatase PP4 negatively regulates type I IFN production and antiviral innate immunity by dephosphorylating and deactivating TBK1. *J. Immunol.* **195**, 3849–3857 (2015).
13. C. S. Friedman, M. A. O'Donnell, D. Legarda-Addison, A. Ng, W. B. Cárdenas, J. S. Yount, T. M. Moran, C. F. Basler, A. Komuro, C. M. Horvath, R. Xavier, A. T. Ting, The tumour suppressor CYLD is a negative regulator of RIG-I-mediated antiviral response. *EMBO Rep.* **9**, 930–936 (2008).
14. L. Zhang, X. Zhao, M. Zhang, W. Zhao, C. Gao, Ubiquitin-specific protease 2b negatively regulates IFN-β production and antiviral activity by targeting TANK-binding kinase 1. *J. Immunol.* **193**, 2230–2237 (2014).
15. D. T. Chalmers, D. P. Behan, The use of constitutively active GPCRs in drug discovery and functional genomics. *Nat. Rev. Drug Discov.* **1**, 599–608 (2002).
16. S. R. George, B. F. O'Dowd, S. P. Lee, G-protein-coupled receptor oligomerization and its potential for drug discovery. *Nat. Rev. Drug Discov.* **1**, 808–820 (2002).
17. E. Alvarez-Curto, G. Milligan, Metabolism meets immunity: The role of free fatty acid receptors in the immune system. *Biochem. Pharmacol.* **114**, 3–13 (2016).
18. Z. Zhang, Z. Wang, H. Ren, M. Yue, K. Huang, H. Gu, M. Liu, B. Du, M. Qian, $P2Y_6$ agonist uridine 5′-diphosphate promotes host defense against bacterial infection via monocyte chemoattractant protein-1-mediated monocytes/macrophages recruitment. *J. Immunol.* **186**, 5376–5387 (2011).
19. A. Ohta, A metabolic immune checkpoint: Adenosine in tumor microenvironment. *Front. Immunol.* **7**, 109 (2016).
20. Y. Yan, W. Jiang, L. Liu, X. Wang, C. Ding, Z. Tian, R. Zhou, Dopamine controls systemic inflammation through inhibition of NLRP3 inflammasome. *Cell* **160**, 62–73 (2015).
21. C. Guo, S. Xie, Z. Chi, J. Zhang, Y. Liu, L. Zhang, M. Zheng, X. Zhang, D. Xia, Y. Ke, L. Lu, D. Wang, Bile acids control inflammation and metabolic disorder through inhibition of NLRP3 inflammasome. *Immunity* **45**, 802–816 (2016).
22. S.-G. Cho, D. Li, K. Tan, S. K. Siwko, M. Liu, KiSS1 and its G-protein-coupled receptor GPR54 in cancer development and metastasis. *Cancer Metastasis Rev.* **31**, 585–591 (2012).
23. W. H. Colledge, GPR54 and puberty. *Trends Endocrinol. Metab.* **15**, 448–453 (2004).
24. S. Funes, J. A. Hedrick, G. Vassileva, L. Markowitz, S. Abbondanzo, A. Golovko, S. Yang, F. J. Monsma, E. L. Gustafson, The KiSS-1 receptor GPR54 is essential for the development of the murine reproductive system. *Biochem. Biophys. Res. Commun.* **312**, 1357–1363 (2003).
25. J. P. Castaño, A. J. Martínez-Fuentes, E. Gutiérrez-Pascual, H. Vaudry, M. Tena-Sempere, M. M. Malagón, Intracellular signaling pathways activated by kisspeptins through GPR54: Do multiple signals underlie function diversity? *Peptides* **30**, 10–15 (2009).
26. T. Iwasa, T. Matsuzaki, A. Tungalagsuvd, M. Munkhzaya, T. Kawami, H. Niki, T. Kato, A. Kuwahara, H. Uemura, T. Yasui, M. Irahara, Hypothalamic Kiss1 and RFRP gene expressions are changed by a high dose of lipopolysaccharide in female rats. *Horm. Behav.* **66**, 309–316 (2014).
27. O. L. Gorbunova, S. V. Shirshev, The role of kisspeptin in immune tolerance formation during pregnancy. *Dokl. Biol. Sci.* **457**, 258–260 (2014).
28. V. M. Navarro, J. M. Castellano, R. Fernández-Fernández, S. Tovar, J. Roa, A. Mayen, R. Nogueiras, M. J. Vazquez, M. L. Barreiro, P. Magni, E. Aguilar, C. Dieguez, L. Pinilla, M. Tena-Sempere, Characterization of the potent luteinizing hormone-releasing activity of KiSS-1 peptide, the natural ligand of GPR54. *Endocrinology* **146**, 156–163 (2005).
29. B. J. Evans, Z. Wang, L. Mobley, D. Khosravi, N. Fujii, J.-M. Navenot, S. C. Peiper, Physical association of GPR54 C-terminal with protein phosphatase 2A. *Biochem. Biophys. Res. Commun.* **377**, 1067–1071 (2008).
30. L. Chevrier, A. de Brevern, E. Hernandez, J. Leprince, H. Vaudry, A. M. Guedj, N. de Roux, PRR repeats in the intracellular domain of KISS1R are important for its export to cell membrane. *Mol. Endocrinol.* **27**, 1004–1014 (2013).
31. Y. Shi, Serine/threonine phosphatases: Mechanism through structure. *Cell* **139**, 468–484 (2009).

32. L. Long, Y. Deng, F. Yao, D. Guan, Y. Feng, H. Jiang, X. Li, P. Hu, X. Lu, H. M. Wang, J. Li, X. Gao, D. Xie, Recruitment of phosphatase PP2A by RACK1 adaptor protein deactivates transcription factor IRF3 and limits type I interferon signaling. *Immunity* **40**, 515–529 (2014).
33. G. M. Cereghetti, A. Stangherlin, O. M. de Brito, C. R. Chang, C. Blackstone, P. Bernardi, L. Scorrano, Dephosphorylation by calcineurin regulates translocation of Drp1 to mitochondria. *Proc. Natl. Acad. Sci. U.S.A.* **105**, 15803–15808 (2008).
34. M. Gu, T. Zhang, W. Lin, Z. Liu, R. Lai, D. Xia, H. Huang, X. Wang, Protein phosphatase PP1 negatively regulates the Toll-like receptor- and RIG-I-like receptor-triggered production of type I interferon by inhibiting IRF3 phosphorylation at serines 396 and 385 in macrophage. *Cell. Signal.* **26**, 2930–2939 (2014).
35. S. Liu, X. Cai, J. Wu, Q. Cong, X. Chen, T. Li, F. Du, J. Ren, Y.-T. Wu, N. V. Grishin, Z. J. Chen, Phosphorylation of innate immune adaptor proteins MAVS, STING, and TRIF induces IRF3 activation. *Science* **347**, aaa2630 (2015).
36. Y. J. Kang, B. Kusler, M. Otsuka, M. Hughes, N. Suzuki, S. Suzuki, W.-C. Yeh, S. Akira, J. Han, P. P. Jones, Calcineurin negatively regulates TLR-mediated activation pathways. *J. Immunol.* **179**, 4598–4607 (2007).
37. R. Nimri, Y. Lebenthal, L. Lazar, L. Chevrier, M. Phillip, M. Bar, E. Hernandez-Mora, N. de Roux, G. Gat-Yablonski, A novel loss-of-function mutation in GPR54/KISS1R leads to hypogonadotropic hypogonadism in a highly consanguineous family. *J. Clin. Endocrinol. Metab.* **96**, E536–E545 (2011).
38. M. G. Teles, S. D. Bianco, V. N. Brito, E. B. Trarbach, W. Kuohung, S. Xu, S. B. Seminara, B. B. Mendonca, U. B. Kaiser, A. C. Latronico, A GPR54-activating mutation in a patient with central precocious puberty. *N. Engl. J. Med.* **358**, 709–715 (2008).
39. X. Liu, M. Yao, N. Li, C. M. Wang, Y. Zheng, X. Cao, CaMKII promotes TLR-triggered proinflammatory cytokine and type I interferon production by directly binding and activating TAK1 and IRF3 in macrophages. *Blood* **112**, 4961–4970 (2008).
40. S. V. Scherbik, M. A. Brinton, Virus-induced Ca^{2+} influx extends survival of west nile virus-infected cells. *J. Virol.* **84**, 8721–8731 (2010).
41. P. R. Beauchesne, N. S. C. Chung, K. M. Wasan, Cyclosporine A: A review of current oral and intravenous delivery systems. *Drug Dev. Ind. Pharm.* **33**, 211–220 (2007).
42. R. J. Firpi, H. Zhu, G. Morelli, M. F. Abdelmalek, C. Soldevila-Pico, V. I. Machicao, R. Cabrera, A. I. Reed, C. Liu, D. R. Nelson, Cyclosporine suppresses hepatitis C virus in vitro and increases the chance of a sustained virological response after liver transplantation. *Liver Transpl.* **12**, 51–57 (2006).
43. M. A. Wainberg, A. Dascal, N. Blain, L. Fitz-Gibbon, F. Boulerice, K. Numazaki, M. Tremblay, The effect of cyclosporine A on infection of susceptible cells by human immunodeficiency virus type 1. *Blood* **72**, 1904–1910 (1988).
44. Z. Shen, H. He, Y. Wu, J. Li, Cyclosporin a inhibits rotavirus replication and restores interferon-beta signaling pathway in vitro and in vivo. *PLOS ONE* **8**, e71815 (2013).
45. J.-P. Liu, L. Ye, X. Wang, J.-L. Li, W.-Z. Ho, Cyclosporin A inhibits hepatitis C virus replication and restores interferon-alpha expression in hepatocytes. *Transpl. Infect. Dis.* **13**, 24–32 (2011).
46. J. Sun, Y. Luan, D. Xiang, X. Tan, H. Chen, Q. Deng, J. Zhang, M. Chen, H. Huang, W. Wang, T. Niu, W. Li, H. Peng, S. Li, L. Li, W. Tang, X. Li, D. Wu, P. Wang, The 11S proteasome subunit PSME3 is a positive feedforward regulator of NF-κB and important for host defense against bacterial pathogens. *Cell Rep.* **14**, 737–749 (2016).
47. M. Kirilov, J. Clarkson, X. Liu, J. Roa, P. Campos, R. Porteous, G. Schütz, A. E. Herbison, Dependence of fertility on kisspeptin-Gpr54 signaling at the GnRH neuron. *Nat. Commun.* **4**, 2492 (2013).
48. A. Rodriguez, J. Roy, S. Martínez-Martínez, M. D. López-Maderuelo, P. Nino-Moreno, L. Orti, D. Pantoja-Uceda, A. Pineda-Lucena, M. S. Cyert, J. M. Redondo, A conserved docking surface on calcineurin mediates interaction with substrates and immunosuppressants. *Mol. Cell* **33**, 616–626 (2009).

Acknowledgments: We thank P. Wang, X. Wang, and D. Xie for plasmids. **Funding:** This work was supported by the National Key R&D Program of China (2018YFA0507000 to B.D.), the National Natural Science Foundation of China (31570896 and 31770969 to B.D. and 81672811 to M.Q.), the Science and Technology Commission of Shanghai Municipality (15JC1401500 to B.D.), the Innovation Program of Shanghai Municipal Education Commission (2017-01-07-00-05-E00011 to M.L.), and the Joint Research Institute for Science and Society (14JORISS01 to B.D.). **Author contributions:** B.D., M.Q., M.L., and H. Huang conceived and designed the experiments. H. Huang, Q.X., N.W., and R.C. performed the experiments. B.D., H. Huang, Q.X., N.W., H. Han, and H.R. analyzed the data. B.D., H. Huang, and S.S. wrote the manuscript. All authors contributed to discussing the results. **Competing interests:** The authors declare that they have no competing interests. **Data and materials availability:** All data needed to evaluate the conclusions in the paper are present in the paper and/or the Supplementary Materials. Additional data related to this paper may be requested from the authors.

Submitted 11 January 2018
Accepted 2 July 2018
Published 8 August 2018
10.1126/sciadv.aas9784

Citation: H. Huang, Q. Xiong, N. Wang, R. Chen, H. Ren, S. Siwko, H. Han, M. Liu, M. Qian, B. Du, Kisspeptin/GPR54 signaling restricts antiviral innate immune response through regulating calcineurin phosphatase activity. *Sci. Adv.* **4**, eaas9784 (2018).

Kisspeptin/GPR54 signaling restricts antiviral innate immune response through regulating calcineurin phosphatase activity

Hongjun Huang, Qingqing Xiong, Ning Wang, Ruoyu Chen, Hua Ren, Stefan Siwko, Honghui Han, Mingyao Liu, Min Qian and Bing Du

Sci Adv **4** (8), eaas9784.
DOI: 10.1126/sciadv.aas9784